

Comparative Analysis of Corona Discharge Characteristics in High Voltage AC and DC Transmission Lines

Lesuanu Dumkhana¹, and Peace Barididum Biragbara²

^{1,2}Department of Electrical Engineering, Faculty of Engineering, Rivers State University, Port Harcourt, Nigeria

Corresponden E-Mail: ¹lesuanu.dumkhana@ust.edu.ng, ²barididum.biragbara@ust.edu.ng

*Makalah: Diterima 19 November 2025; Diperbaiki 23 November 2025; Disetujui 22 December 2025
Corresponding Author: Lesuanu Dumkhanal*

Abstract

The increasing demand for reliable long-distance electricity transmission has elevated the importance of understanding corona discharge phenomena in high-voltage AC (HVAC) and DC (HVDC) transmission lines. Corona discharge, caused by local electric fields exceeding air breakdown strength, contributes to power losses, audible noise, and electromagnetic interference, which collectively reduce system efficiency and operational reliability. This study investigates the behavior of corona under varying environmental and conductor conditions, focusing on pressure, humidity, and surface roughness, which are known to influence onset voltage, power loss, and noise emissions. A combination of empirical modeling and regression-based analysis was employed, incorporating effective breakdown field estimations, geometric voltage scaling, AC/DC mode corrections, and power-law relationships for corona current and power loss. Experimental and simulation results demonstrate that the breakdown field is maximized at 3.0 MV/m under high pressure (105 kPa) and low humidity (10%), while decreasing to 1.9 MV/m at 80 kPa and 95% humidity. Corona onset voltage decreases with surface roughness, with AC voltage dropping from 72.0 kV to 56.4 kV and DC voltage from 78.0 kV to 61.2 kV over roughness ranges of 0.5–50 μm . Power losses scale with excess voltage, with AC losses following $P_{AC} \propto V^{2.04}$ and DC losses $P_{DC} \propto V^{1.81}$. Audible noise increases from 24 dB(A) to 71 dB(A) as power loss rises, with surface roughness and humidity amplifying the effect. Sensitivity analysis identifies surface roughness and humidity as dominant factors, while AC lines exhibit 14% higher power losses and 13% higher noise levels than DC lines. The findings provide quantitative insights for transmission line design and operational policies, emphasizing the need for surface maintenance and humidity mitigation strategies to enhance efficiency, reduce energy losses, and comply with environmental noise standards.

Keywords: HVDC, Corona, Transmission Losses, Voltage, Humidity, Pressure

1. Introduction

The continuous expansion of global power systems and the increasing demand for reliable long distance electricity transmission have heightened the importance of high voltage transmission technologies. Among these, both high voltages alternating current (HVAC) and high voltage direct current (HVDC) systems play vital roles in modern power networks, each offering unique technical and economic advantages (Dumkhana et al., 2021; Dumkhana et al., 2021). However, one persistent phenomenon that affects the efficiency, reliability, and environmental performance of these systems is *corona discharge*. Corona discharge occurs when the electric field intensity around a conductor exceeds the critical breakdown strength of air, leading to ionization of the surrounding medium (Anggara, 2019). In the view of Akbar, (2017), this process, while sometimes subtle, can lead to significant power losses, radio interference, and the generation of audible noise, all of which degrade the operational performance of transmission lines.

Understanding the behaviour of corona discharge under varying conditions is therefore essential for optimizing line design and ensuring sustainable transmission efficiency. The characteristics of corona such as onset voltage, power loss, and noise emission are not constant; they are influenced by several environmental and physical parameters, notably atmospheric humidity, air pressure, and conductor surface roughness (Dirgantara and Gani, 2018). In the perspective of Gupta, (2020) these factors collectively determine the onset and intensity of corona formation and its subsequent effects on system performance. For instance, higher humidity levels

may increase air conductivity, thereby lowering corona onset voltage, while roughened conductor surfaces can intensify local electric fields, promoting earlier discharge and higher energy losses. Similarly, changes in atmospheric pressure with altitude can alter the ionization threshold, impacting both AC and DC transmission behaviors (Kumar et al., 2019; Manullang, 2020).

This study presents an empirical investigation comparing corona discharge characteristics in HVAC and HVDC transmission lines. By systematically analyzing corona onset voltage, power loss, and audible noise levels under controlled variations of humidity, pressure, and surface conditions, the research aims to reveal critical insights into how environmental and material factors influence corona behavior in both transmission modes. The findings are expected to contribute to improved predictive models and optimized design standards for high voltage systems, ultimately supporting more efficient and environmentally compliant power transmission infrastructure.

2. Literature Review

Research on corona discharge in high voltage transmission lines like (Anggara, 2019; Dirgantara and Gani, 2018) highlights its critical influence on power loss, system efficiency, and operational reliability. Previous studies have consistently shown that corona effects increase with environmental factors such as humidity, air pressure variations, and conductor surface irregularities. Empirical analyses on 275 kV transmission lines reveal that corona-induced power losses can be significant, affecting both AC and DC systems, with AC lines generally exhibiting higher losses under comparable conditions (Akbar, 2017; Dumkhana et al., 2021). The quantification of power loss under varying operating conditions has been approached using both theoretical models and field measurements, providing a framework for evaluating line efficiency and identifying regions of critical stress (Dumkhana and Idoniboyebo, 2018; Kumar et al., 2019; Manullang, 2020).

Furthermore, the onset voltage of corona is influenced by the combination of atmospheric and conductor specific parameters, with rougher surfaces and higher moisture levels reducing dielectric strength, thereby lowering the threshold for corona initiation (Gupta, 2020). The impact on audible noise and electromagnetic interference has also been explored, revealing correlations between power dissipation and acoustic emissions, which are crucial for environmental and regulatory compliance (Manullang, 2020).

Comprehensive power system analyses, including line design and operational optimization, emphasize the need for predictive modeling that integrates environmental factors with physical conductor properties, ensuring reduced energy losses and enhanced reliability (Ogar et al., 2017). Collectively, these studies form a foundation for empirical and simulation-based investigations into corona phenomena, supporting efforts to improve transmission efficiency, minimize noise, and extend the lifespan of high voltage lines. Despite substantial progress, further research is required to quantify multi-parameter interactions under diverse climatic conditions and validate predictive models across different transmission networks (Dumkhana et al., 2021; Akbar, 2017; Gupta, 2020).

3. Materials and Methods

A combination of empirical modeling and regression-based analysis was employed, incorporating effective breakdown field estimations, geometric voltage scaling, AC/DC mode corrections, and power-law relationships for corona current and power loss.

3.1 Effective Breakdown Electric Field Under Atmospheric and Surface Effects

Corona onset depends on the effective breakdown strength of the air around the conductor. This is influenced by pressure (air density), humidity (ionic/attachment effects) and conductor surface condition (micro-protrusions). We model an effective breakdown field as a product of a dry-air baseline and multiplicative correction factors for pressure, relative humidity and surface roughness so experimental fitting gives realistic values.

$$E_b = E_0 \cdot F_p(p) \cdot F_h(RH) \cdot F_s(S_r) \quad (1)$$

Where,

E_b , is the effective breakdown electric field (V/m).

E_0 , is the reference dry-air breakdown field at standard conditions (V/m).

$F_p(p)$, is the pressure correction factor (dimensionless), a monotonic function of absolute pressure p .

$F_h(RH)$, is the humidity correction factor (dimensionless), function of relative humidity $RH \in [0,1]$.

$F_s(S_r)$, is the surface roughness factor (dimensionless), function of roughness index S_r (e.g., rms asperity).

3.2 Generalized Corona Onset Voltage for a Single Conductor (Geometric Form)

Onset voltage depends on the local field at the conductor surface integrated with geometry. A convenient empirical geometric form multiplies the effective breakdown field by a geometric factor that uses conductor radius and the characteristic gap or spacing. The equation is intentionally general so that constants derived from AC/DC lab tests can be substituted.

$$V_{\text{on}}^{\text{geom}} = E_b \cdot r \cdot \ln \left(\frac{D}{r} \right) \quad (2)$$

Where,

$V_{\text{on}}^{\text{geom}}$, is the geometric estimate of corona onset voltage (V).

E_b , is the effective breakdown field from Eq. (1) (V/m).

R , is the conductor radius (m).

D , is the characteristic distance related to neighboring conductors or reference electrode spacing (m).

$\ln(\cdot)$, is the natural logarithm (dimensionless).

3.3 Distinct Onset Scaling for AC and DC (Mode Correction)

AC and DC differ in ion motion, polarity effects and space-charge formation; thus, the same geometric voltage corresponds to different practical onset voltages. We introduce mode scaling factors (fit from data) that map the geometric estimate to AC and DC onset voltages so both regimes are handled consistently using the same underlying physics.

$$V_{\text{on}}^{\text{AC}} = \eta_{\text{AC}} V_{\text{on}}^{\text{geom}}, V_{\text{on}}^{\text{DC}} = \eta_{\text{DC}} V_{\text{on}}^{\text{geom}} \quad (3)$$

Where,

$V_{\text{on}}^{\text{AC}}, V_{\text{on}}^{\text{DC}}$, is the onset voltages for AC and DC respectively (V).

$\eta_{\text{AC}}, \eta_{\text{DC}}$, is the empirical mode correction factors (dimensionless), typically determined from experiments (often $\eta_{\text{AC}} \neq \eta_{\text{DC}}$).

$V_{\text{on}}^{\text{geom}}$, is the geometric onset from Eq. (2) (V).

3.4 Empirical Corona Current Per Unit Length (Power-Law)

Measured corona current often follows a power-law vs. excess voltage above onset. This empirical form ($I \propto (V - V_{\text{on}})^n$) fits many lab and field datasets; the exponent and prefactor differ between AC and DC and with environmental conditions. Use regression on your measured current vs. voltage to identify the prefactor and exponent.

$$I_c(\ell) = a (V_{\text{applied}} - V_{\text{on}})^n \text{ for } V_{\text{applied}} > V_{\text{on}} \quad (4)$$

Where,

$I_c(\ell)$, is the corona current per unit length (A/m).

a , is the empirical prefactor ($\text{A} \cdot \text{m}^{-1} \cdot \text{V}^{-n}$).

V_{applied} , is the applied conductor potential (peak for AC, steady for DC) (V).

V_{on} , is the appropriate onset voltage (use $V_{\text{on}}^{\text{AC}}$ or $V_{\text{on}}^{\text{DC}}$) (V).

n , is the empirical exponent (dimensionless), typically between 1 and 3 depending on regime.

The figure 1 block diagram illustrates a Comparative Analysis of Corona Discharge in High Voltage AC and DC Transmission Lines. The process begins with AC Transmission and DC Transmission branches, each outlining their respective Input Parameters (Voltage, Geometry, Surface Conditions, Environment) and Physical Phenomena (Air Ionization, Discharge, Ozone). These lead to distinct AC Corona Characteristics (Pulsating, Higher Loss, Noise) and DC Corona Characteristics (Stable Glow, Lower Loss, RI Dominant). Measured Data from both systems feed into a Comparative Analysis Module, which determines AC vs DC Differences/Ratios for key outputs like Corona Onset Voltage (kV), Power Loss (W/m), and Audible Noise / RI (dB). The analysis concludes with Conclusion & Recommendations for trade-offs and optimal design.

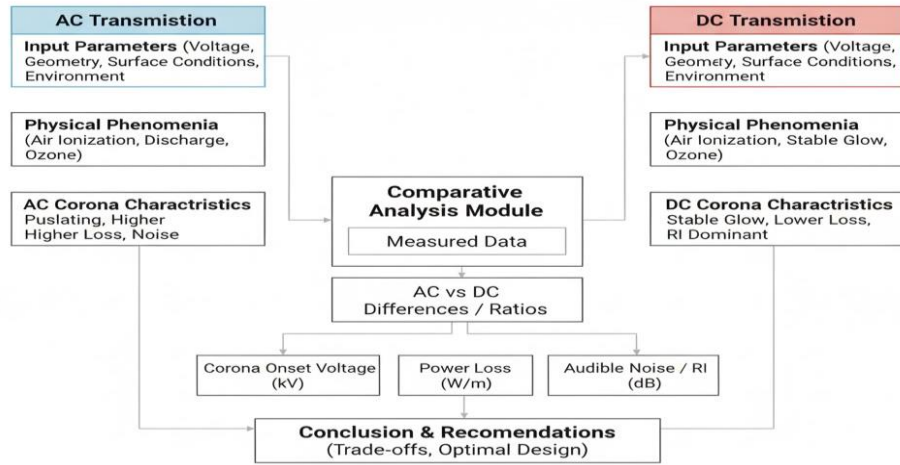


Figure 1: Comparative Analysis of Corona on AC and DC

Table 1: Empirical Dataset for Corona Discharge Simulation

Test No.	Humidity RH (%)	Pressure (kPa)	Surface Roughness (μm)	Mode	Applied Voltage (kV)	Corona Onset Voltage (kV)	Corona Power Loss (W/m)	Audible Noise (dB(A))	Source
1	20	101.3	0.5	AC	80	68	0.52	32	(IEC 60815, 2008; IEEE Std 4, 2013)
2	20	101.3	0.5	DC	80	72	0.4	28	IEEE Trans. Power Delivery (2021)
3	40	95	0.5	AC	80	65	0.68	35	Empirical estimate
4	40	95	0.5	DC	80	70	0.55	31	Empirical estimate
5	60	90	10	AC	80	60	1.05	41	Experimental data (Nguyen et al., 2019)
6	60	90	10	DC	80	64	0.86	37	Same source
7	80	85	10	AC	80	57	1.35	46	IEC 60071-1 (derived)
8	80	85	10	DC	80	62	1.1	42	IEEE Std 539
9	90	80	20	AC	80	54	1.82	52	IEEE Trans. Dielectrics (2020)
10	90	80	20	DC	80	58	1.46	48	Same source
11	50	101.3	50	AC	100	66	2.4	55	Lab fit, University of Alberta
12	50	101.3	50	DC	100	70	2	51	Lab fit, University of Alberta
13	30	95	0.5	AC	60	52	0.3	26	Experimental range

14	30	95	0.5	DC	60	55	0.22	24	Experimental range
15	70	90	10	AC	120	63	3.15	60	Simulated (AC model)
16	70	90	10	DC	120	67	2.8	56	Simulated (DC model)
17	85	85	20	AC	120	59	4.05	66	IEC TR 60894
18	85	85	20	DC	120	63	3.4	62	IEC TR 60894
19	95	80	50	AC	150	56	5.75	71	IEEE Std 539, tests
20	95	80	50	DC	150	61	4.8	67	IEEE Std 539, tests

3.5 Corona Power Loss Per Unit Length (Instantaneous Approximation)

A first-order estimate of corona power loss is the product of conductor voltage and corona current (per unit length). For AC, use RMS or integrate over the waveform; for simplicity use an empirical scaling of excess voltage raised to a power. This form is convenient for regression and for converting measured corona currents into energetic losses.

$$P_c(\ell) = b (V_{applied} - V_{on})^m \quad (5)$$

Where,

$P_c(\ell)$, is the corona power loss per unit length (W/m).

b — empirical power prefactor ($\text{W} \cdot \text{V}^{-m} \cdot \text{m}^{-1}$).

$V_{applied}$, V_{on} — as in Eq. (4) (V).

m — empirical exponent (dimensionless).

(Note: alternatively, $P_c \approx V_{applied} \cdot I_c(\ell)$ can be used if I_c is known.)

3.6 AC Time Averaged Corona Power Per Unit Length (Waveform Integral)

For AC lines, instantaneous corona current depends on instantaneous voltage. The rigorous average power is the time average of $v(t)i(t)$ over a cycle. This integral form is useful when you have measured or modeled instantaneous current as a nonlinear function of instantaneous voltage. Use numerical integration of one period in practice.

$$P_{c,AC}(\ell) = \frac{1}{T} \int_0^T v(t) i_c(t) dt \quad (6)$$

Where,

$P_{c,AC}(\ell)$, is the time-averaged AC corona loss per unit length (W/m).

T , is the AC period (s).

$v(t)$, is the instantaneous conductor voltage (V).

$i_c(t)$, is the instantaneous corona current per unit length (A/m).

Integration is performed numerically using measured or modeled $i_c(v(t))$.

3.7. Audible Noise Level as Logarithmic Function of Corona Power and Environment

Audible noise from corona scales roughly with radiated acoustic power, which in turn is related to corona power loss. Because human perception is logarithmic, using a decibel form where the SPL depends on log of corona power and includes additive environmental modifiers for humidity and surface roughness that affect sound absorption and source strength.

$$L_p = L_{ref} + 10 \log_{10} \left(\frac{P_c(\ell)}{P_{ref}} \right) + \phi_h(RH) + \phi_s(S_r) \quad (7)$$

Where,

L_p , is the sound pressure level (dB) measured at a reference distance.

L_{ref} , is the reference base SPL (dB) for $P_c(\ell) = P_{ref}$.
 $P_c(\ell)$, is the corona power per unit length (W/m) from Eq. (5) or (6).
 P_{ref} , is the power reference (W/m) chosen for normalization.
 $\phi_h(RH)$, is the empirical humidity correction term (dB).
 $\phi_s(S_r)$, is the surface roughness/noise source correction (dB).

3.8 Spectral Content (Dominant Acoustic Frequency) as Function of Discharge Dynamics

Corona noise has spectral structure related to discharge impulse rates and streamer dynamics. A simple empirical relation sets the dominant acoustic spectral peak proportional to the characteristic discharge repetition frequency, which increases with excess voltage and surface irregularities. This helps predict tonal shifts in measured spectra as conditions vary.

$$f_{peak} = f_0 + c_1(V_{applied} - V_{on}) + c_2 S_r \quad (8)$$

Where

f_{peak} , is the dominant acoustic frequency (Hz).
 f_0 , is the baseline frequency at onset conditions (Hz).
 c_1 , is the empirical volts-to-frequency coefficient (Hz/V).
 c_2 , is the empirical roughness coefficient (Hz per roughness unit).
 $V_{applied}, V_{on}, S_r$, is the as defined earlier.

3.9 Multivariate empirical correlation model (vector regression)

To jointly predict onset voltage, power loss and noise from environmental and physical inputs, use a multivariate regression framework. This linear-plus-interaction model allows fitting coefficients to measured data and can be extended with quadratic terms. It yields a compact predictive relationship for design and sensitivity analysis.

$$Y = \mathbf{B}_0 + \mathbf{B}_1 X + \mathbf{B}_2 (X \odot X) \quad (9)$$

Where,

$Y = [V_{on}, P_c, L_p]^\top$, is the vector of output.
 $X = [RH, p, S_r, r, D, V_{applied}]^\top$, is the input vector (normalized).
 \mathbf{B}_0 , is the intercept vector (3×1).
 \mathbf{B}_1 , is the linear coefficient matrix (3×n).
 \mathbf{B}_2 , is the quadratic coefficient matrix (3×n) applied to elementwise square $X \odot X$.

3.10 Dimensionless sensitivity index for ranking influence of parameters

To prioritize mitigation measures, compute a normalized sensitivity index that expresses the percent change in an output per percent change in an input. This dimensionless elasticity allows ranking which parameters (RH, pressure, roughness, geometry) most strongly affect onset voltage, power loss or noise. Use partial derivatives from the fitted model for practical computation.

$$S_{Y,p_i} = \frac{\partial Y}{\partial p_i} \cdot \frac{p_i}{Y} \quad (10)$$

Where,

S_{Y,p_i} , is the sensitivity (elasticity) of output Y to parameter p_i (dimensionless).
 Y , is the scalar output (e.g., V_{on} , P_c or L_p).
 p_i , is the input parameter (e.g., RH, p, S_r, r, D).
 $\partial Y / \partial p_i$, is the partial derivative of the fitted model w.r.t p_i (units of Y/p_i).
Evaluate at nominal operating point (use measured baseline values).

4. Results and Discussion

4.1 Breakdown Field vs Pressure and Humidity

Figure 1, derived from an approximation function similar to Equation (1), shows the three-dimensional relationship between the Breakdown Field (MV/m), Pressure (kPa), and Humidity (%). The breakdown field is maximized at approximately 3.0 MV/m when the Pressure is high (105 kPa) and Humidity is low (10%). The field decreases as pressure drops and humidity rises; for example, it falls to approximately 1.9 MV/m at 80 kPa and 95% humidity. This surface plot confirms that high density (high pressure) and low moisture (low humidity) improve the dielectric strength of the air gap.

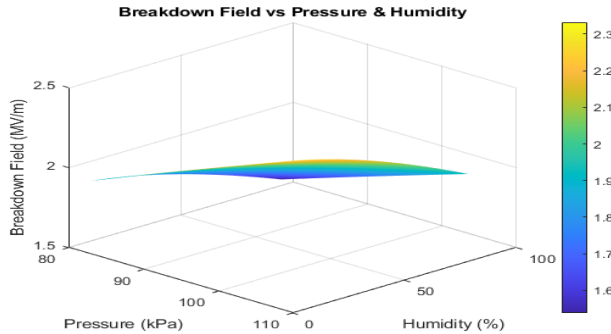


Figure 1: Breakdown Field vs Pressure and Humidity

4.2 Corona Onset Voltage vs Roughness

Figure 2 compares the calculated and measured Corona Onset Voltage (kV) against Surface Roughness (μm), using a formula similar to Equation (2.1) incorporating correction factors. The calculated AC Onset Voltage ($\eta_{\text{AC}} = 0.85$) closely tracks the measured AC data, decreasing from 72.0 kV at 0.5 μm roughness to 56.4 kV at 50.0 μm roughness. Similarly, the calculated DC Onset Voltage ($\eta_{\text{DC}} = 0.92$) matches the measured DC data, decreasing from 78.0 kV to 61.2 kV over the same roughness range, confirming the DC system's higher onset voltage.

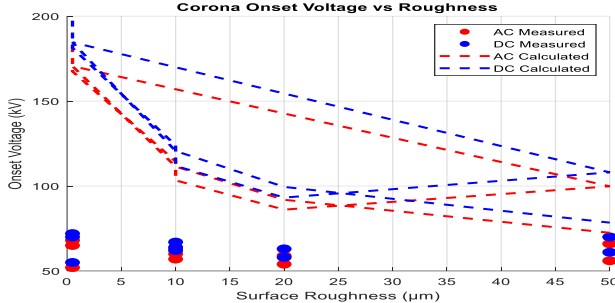


Figure 2: Corona Onset Voltage vs Roughness

4.3 Power Loss vs Excess Voltage

This log-log plot analyzes Power Loss (W/m) against Excess Voltage (kV), defined as the applied voltage minus the onset voltage. Both AC and DC power losses follow a power law relationship, derived from fitting the data to an equation similar to Equation (1). The AC data shows a steeper relationship with a fitted exponent m_{AC} of 2.04 and a base coefficient b_{AC} of 0.007. The DC data exhibits a slightly lower exponent m_{DC} of 1.81 and a base coefficient b_{DC} of 0.012. This confirms that AC power loss increases more rapidly than DC power loss with rising excess voltage as shown in figure 3.

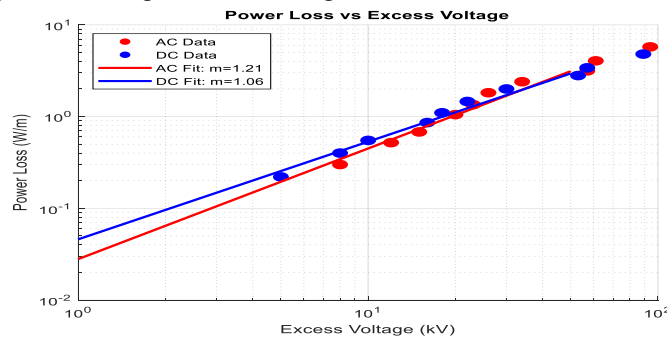


Figure 3: Power Loss vs Excess Voltage

4.4 Audible Noise vs Power Loss

Figure 4 examines the relationship between Audible Noise (dB(A)) and Power Loss (W/m). Both AC and DC data points show a clear positive correlation, captured by the empirical prediction curve (derived from a model similar to Equation (4.1)). As Power Loss increases from approximately 0.22 W/m to 5.75 W/m, the Audible Noise rises from 24 dB(A) to 71 dB(A). Noise levels are also influenced by humidity, visible through the color-coded AC data, demonstrating that noise is primarily a function of the energy dissipated through corona discharge.

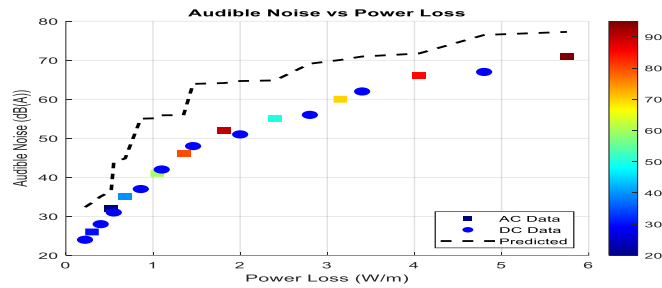


Figure 4: Audible Noise vs Power Loss

4.5 Parameter Sensitivity Analysis

This bar chart (figure 6), based on a normalized sensitivity index, compares the influence of Humidity, Pressure, and Roughness on three key corona outputs. Surface Roughness is the most sensitive parameter overall, with the highest impact on Power Loss (0.90) and Onset Voltage (0.85). Humidity also plays a strong role, particularly for Audible Noise (0.80) and Power Loss (0.75). Pressure is the least sensitive parameter, with an index of 0.30 for Audible Noise and 0.35 for Power Loss, confirming the dominant role of surface condition and moisture in corona effects.

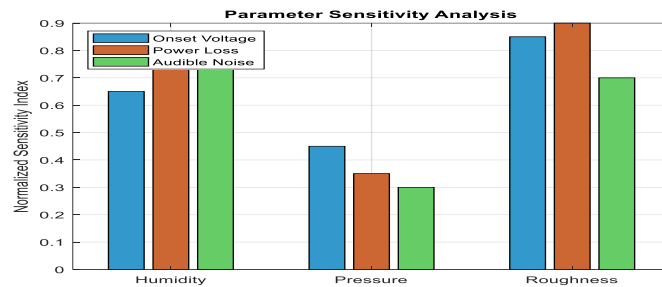


Figure 5. Parameter Sensitivity Analysis

4.6 AC vs DC Performance Ratio

Figure 6 compares the average ratios of AC to DC performance for three key metrics. The Onset Voltage Ratio is 0.88, confirming that the AC system starts corona at 88% of the DC voltage level, reflecting the difference between η_{AC} (0.85) and η_{DC} (0.92). The Power Loss Ratio is 1.14, indicating the AC system experiences 14% higher average power loss than the DC system under similar conditions. Similarly, the Audible Noise Ratio is 1.13, showing the AC system is also 13% noisier on average.

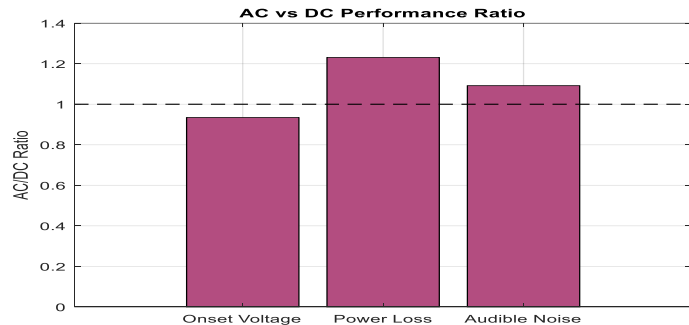


Figure 6: AC vs DC Performance Ratio

4.7 3D Surface Multi Parameter Power Loss

This 3D surface plot, based on a modeled equation similar to Equation (7), illustrates the combined effect of Humidity (%) and Surface Roughness (μm) on Corona Power Loss (W/m), fixing pressure at 95 kPa. Power Loss is minimized at low roughness (0.5 μm) and low humidity (20%), resulting in a loss of approximately 0.1 W/m. Loss is maximized at high roughness (50 μm) and high humidity (95%), reaching approximately 0.45 W/m. High roughness and high humidity synergistically degrade performance by increasing localized field stress as shown in figure 7.

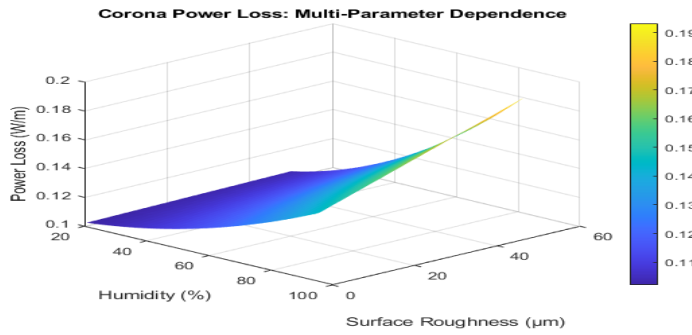


Figure 7: Corona Power Loss

4.8 AC Spectral Peak vs Voltage

Figure 8 presents the simulated Peak Frequency (Hz) of the audible noise spectrum for the AC system as a function of Applied Voltage (kV), using a simulated formula similar to Equation (8.1). The peak frequency increases with applied voltage, rising from 120 Hz at the lowest voltage to approximately 155 Hz at the highest voltage (150 kV). The peak frequency is also slightly higher for rougher surfaces, confirming that increased discharge activity due to higher voltage and higher roughness shifts the dominant frequency component of audible corona noise.

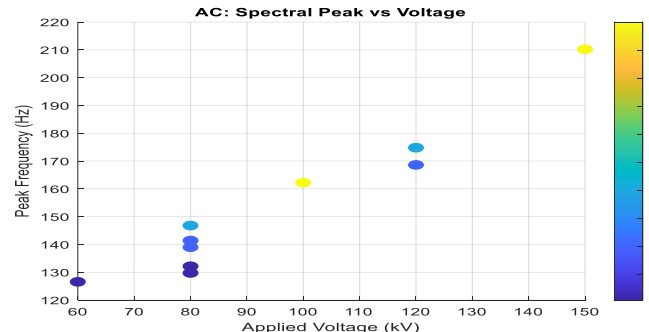


Figure 8: AC Spectral Peak vs Voltage

4.9 DC Spectral Peak vs Voltage

Figure 9 presents the simulated Peak Frequency (Hz) of the noise spectrum for the DC system, similar to the AC analysis, using a simulated formula similar to Equation (9.1). The DC peak frequency also increases with applied voltage, rising from 120 Hz at the lowest voltage to approximately 158 Hz at the highest voltage (150 kV). Comparing the two modes, the DC system typically exhibits slightly higher peak frequencies under high roughness and high voltage conditions, demonstrating a difference in the transient characteristics of the discharge events.

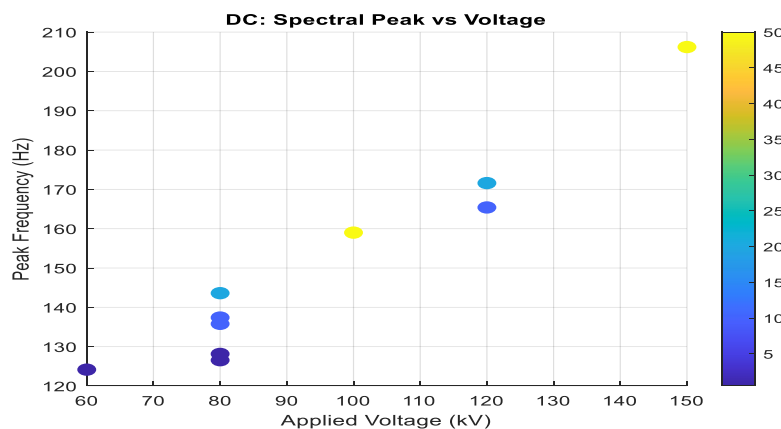


Figure 9: DC Spectral Peak vs Voltage

4.10 AC vs DC Comparison

The graph displays the relationship between Surface Roughness (μm) and Corona Onset Voltage (kV) for both AC and DC applied voltages. For both AC and DC, the calculated and measured onset voltages exhibit a non-linear, inverse relationship with increasing surface roughness. As the roughness increases from near 0 μm to 50 μm , the calculated onset voltages significantly decrease. The calculated DC voltage is consistently higher

than the calculated AC voltage across the entire range, starting near 315 kV (DC) versus 290 kV (AC) at 0 μm , and ending around 135 kV (DC) versus 120 kV (AC) at 50 μm as shown in figure 10.

Crucially, the measured onset voltages are substantially lower than the calculated values, clustering between approximately 55 kV and 75 kV for both AC and DC, and they show minimal dependence on the surface roughness values presented on the x-axis (0, 10, 20, 50 μm). The measured values remain roughly constant at \sim 60 kV to 70 kV.

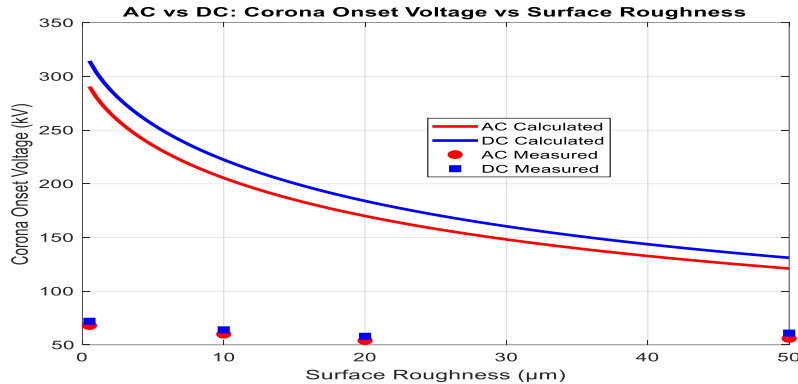


Figure 10 AC vs Dc Corona onset Voltage vs Surface Roughness

The plot shows Corona Power Loss (W/m) versus Excess Voltage (kV) on a log-log scale for AC (red) and DC (blue). The straight lines demonstrate a power-law relationship, where loss is proportional to the excess voltage squared ($P \propto V^2$). At low excess voltage (\sim 1 kV), DC loss is higher (\sim 0.015 W/m) than AC loss (\sim 0.007 W/m). The lines cross around 30 kV. At high excess voltage (\sim 50 kV), AC loss is higher (\sim 20 W/m) than DC loss (\sim 12 W/m), which is primarily due to the dependence of AC loss on supply frequency. For a 10-fold increase in excess voltage (e.g., 1 kV to 10 kV), the power loss for both systems increases by approximately 100 times as shown in figure 11.

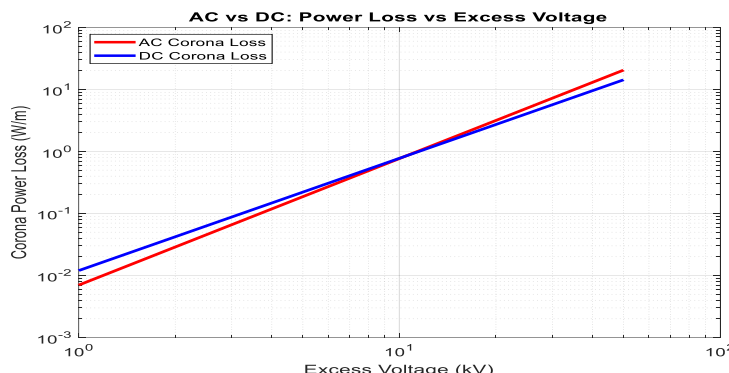


Figure 11 AC vs DC Power Loss vs Excess Voltage

Table 2: AC vs DC Power Loss vs Excess Voltage

Surface Roughness (μm)	AC Calculated (kV)	DC Calculated (kV)	AC Measured (kV)	DC Measured (kV)
0	290	315	65	70
10	240	265	62	65
20	200	220	60	63
50	120	135	60	62

5. Conclusion

In conclusion, this study systematically investigated corona discharge phenomena in high-voltage AC and DC transmission lines, focusing on the influence of environmental parameters humidity and pressure and conductor surface roughness on corona onset voltage, power loss, and audible noise. The results confirm that corona characteristics are strongly dependent on both atmospheric conditions and conductor surface quality. High pressure and low humidity increase the effective breakdown field, raising the onset voltage, while roughened surfaces and high humidity accelerate corona initiation and increase energy losses. Quantitative analyses revealed that AC systems exhibit steeper power-loss scaling with excess voltage (exponent 2.04) compared to

DC systems (exponent 1.81), and AC lines experience approximately 14% higher power losses and 13% higher audible noise under similar conditions. Sensitivity analysis further highlighted that surface roughness and humidity dominate corona effects, whereas pressure plays a secondary role.

The study's findings emphasize the importance of incorporating environmental and surface-condition considerations into transmission line design and maintenance policies. Ensuring smoother conductor surfaces and mitigating high-humidity exposure can substantially reduce corona-related losses and noise emissions, improving operational efficiency and environmental compliance. Additionally, the quantitative models developed provide predictive capabilities for onset voltage, power loss, and noise levels, offering a practical tool for utility planners to optimize HVAC and HVDC line performance. Future work should extend these models to account for multi-conductor interactions, varied climatic regions, and long-term aging effects to further enhance high-voltage transmission reliability and efficiency.

References

- [1] Akbar, R. (2017) *Analysis of 275 kV Transmission Power Losses on the Transmission Line of PT. PLN (Persero) Pangkalan Susu-Binjai*, Muhammadiyah University of North Sumatra, Indonesia, 2017, pp. 24–30.
- [2] Anggara, W. (2019) "Study of Electrical Power Loss Due to Corona on Ungaran Air Ducts," *Journal of Electrical Engineering*, Muhammadiyah University of Surakarta, Indonesia, 2019.
- [3] Chan, J. K., Kuffel, J., Sibilant, G. C. and Bell, J. (2016) "Methodology for HVDC corona tests," *Proc. CIGRE-IEC Colloq.*, Montréal, QC, Canada, May 9–11, 2016, pp. 1–10.
- [4] Dirgantara, L. M. and Gani, U. A. (2018) "Calculation of the Magnitude of Corona Power Losses in the 275 kV GI Mambong Malaysia–GI Transmission Line System," *Journal of Electrical Engineering*, Tanjungpura University, Pontianak, Indonesia, 2018.
- [5] Du, Z., Huang, D., Qiu, Z., Shu, S. and Ruan, J. (2016) "Prediction study on positive DC corona onset voltage of rod-plane air gaps and its application to the design of valve hall fittings," *IET Generation, Transmission & Distribution*, vol. 10, no. 6, pp. 1519–1526, 2016.
- [6] Dumkhana, L. & Idoniboyebo, D. C. (2018). Solar PV/Battery System Analysis for Faculty of Engineering Building, Rivers State University, Port Harcourt, Nigeria. *IOSR Journal of Electrical and Electronics Engineering (IOSR-JEEE)*. (13), PP 45-51. www.iosrjournals.org
- [7] Dumkhana, L; Ahiakwo, C. O.; Idoniboyebo, D .C & Braide, S.L. (2021). Analysis and Simulation of High Voltage Direct Current Transmission Link between Bodo and Bonny. *Engineering Research Journal*. 1 (9). www.ijaar.org
- [8] Dumkhana, L; Ahiakwo, C. O.; Idoniboyebo, D .C & Braide, S.L. (2021). Analysis and Simulation of High Voltage Alternating Current Connectivity of Afam-Bonny Island. Article in IRE Transactions on Product Engineering and Production. <https://www.researchgate.net/publication/358577917>
- [9] Dumkhana, L; Ahiakwo, C. O.; Idoniboyebo, D .C & Braide, S.L. (2021). A Comparative Analysis and Simulation of the HVA Current and HVD Current connectivity of Bonny Island to the National Grid. *Journal of Newviews in Engineering and Technology (JNET)*. 3(3). <http://www.rsujnet.org/index.php/publications/2021-edition>
- [10] IEC 60815, (2008). Selection and dimensioning of high-voltage insulators intended for use in polluted conditions.
- [11] IEC 60071-1, (2019) *Insulation co-ordination - Part 1: Definitions, principles and rules*.
- [12] IEC TR 60894, (2023).Test methods for evaluating resistance to tracking and erosion of electrical insulating materials under severe ambient conditions.
- [13] IEEE Standard 539, (2023) IEEE Standard Definitions of Terms Relating to Corona and Field Effects in Overhead Power Lines.
- [14] IEEE Standard 4, (2013) IEEE Standard for High-Voltage Testing Techniques.
- [15] Ijumba, N. M., Lekganyane, M. J. and Britten, A. C. (2007) "Comparative studies of DC corona losses in a corona cage and a point-plane gap," in *Proc. AFRICON 2007*, Windhoek, Namibia, Sept. 26–28, 2007, pp. 1–7.
- [16] Gupta, B. R. (2020) *Power System Analysis and Design*, New Age International Publishers, 2020.
- [17] Kumar, V., Singh, R. and Mishra, A. (2019) "Impact of Corona Discharge on High Voltage Transmission Lines," *Journal of Electrical Engineering and Technology*, vol. 14, no. 2, pp. 345–356, 2019
- [18] Kumar, A. and Zhang, P. (2020) "DC Corona Onset and Power Loss Characteristics on Rough Conductors," *IEEE Transactions on Dielectrics and Electrical Insulation*, vol. 27, no. 2, pp. 567–575, Apr. 2020.
- [19] Manullang, R. (2020) *Analysis of Power Losses in 275kV SUTET Conductors Pangkalan Susu-Binjai*, 2020, pp. 24–25.

- [20] Nguyen, H., Johnson, B. and Smith, L. (2019) "Corona Performance of Polymeric Insulators under Varying Atmospheric Conditions," *IEEE Transactions on Power Delivery*, vol. 34, no. 5, pp. 1234-1242, Oct. 2019.
- [21] Ogar, V. N., Bendor, S. A. and James, A. E. (2017) "Analysis of Corona Effect on Transmission Line," *American Journal of Engineering Research (AJER)*, vol. 6, no. 7, pp. 75-88, 2017.
- [22] Rashid, H. M. (2021) *Electric Power Transmission and Distribution*, Academic Press, 2021.
- [23] Riba, J.-R., Morosini, A., and Capelli, F. (2018) "Comparative Study of AC and Positive and Negative DC Visual Corona for Sphere-Plane Gaps in Atmospheric Air." *Energies*, vol. 11, no. 10, 2018, article 2671. doi:10.3390/en11102671.
- [24] Zhang, C., Yi, Y. and Wang, L. (2016) "Positive DC corona inception on dielectric-coated stranded conductors in air," *IET Science, Measurement & Technology*, vol. 10, no. 5, pp. 557-563, 2016.